Nonisothermal Crystallization Kinetics of Poly(butylene terephthalate)/Montmorillonite Nanocomposites

Defeng Wu,[1] Chixing Zhou,[1] Xie Fan,[1] Dalian Mao,[2] Zhang Bian[2]

[1]*School of Chemistry & Chemical Technology, Shanghai Jiaotong University, Shanghai 200240, China*
[2]*Nantong XinChen Synthetic Material Company, Limited, Jiangsu 226006, China*

ABSTRACT: The melt intercalation method was employed to prepare poly(butylene terephthalate) (PBT)/montmorillonite (MMT) nanocomposites, and the microstructures were characterized with X-ray diffraction and transmission electron microscopy. Then, the nonisothermal crystallization behavior of the nanocomposites was studied with differential scanning calorimetry (DSC). The DSC results showed that the exothermic peaks for the nanocomposites distinctly shifted to lower temperatures at various cooling rates in comparison with that for pure PBT, and with increasing MMT content, the peak crystallization temperature of the PBT/MMT hybrids declined gradually. The nonisothermal crystallization kinetics were analyzed by the Avrami, Jeziorny, Ozawa, and Mo methods on the basis of the DSC data. The results revealed that very small amounts of clay (1 wt %) could accelerate the crystallization process, whereas higher clay loadings reduced the rate of crystallization. In addition, the activation energy for the transport of the macromolecular segments to the growing surface was determined by the Kissinger method. The results clearly indicated that the hybrids with small amounts of clay presented lower activation energy than PBT, whereas those with higher clay loadings showed higher activation energy. The MMT content and the crystallization conditions as well as the nature of the matrix itself affected the crystallization behavior of the hybrids. © 2006 Wiley Periodicals, Inc. J Appl Polym Sci 99: 3257–3265, 2006

Key words: crystallization; kinetics (polym.); nanocomposites

INTRODUCTION

Poly(butylene terephthalate) (PBT), a typical semicrystalline polymer, is an engineering plastic with excellent mechanical properties that has found wide applications in the fields of fibers and nonfibers. There has been much research on modifying PBT, and studies have been mainly focused on blending PBT with other polymers or fillers to obtain new polymeric materials with desirable properties.[1–5]

In recent years, nanocomposites based on organic polymers and inorganic clay minerals consisting of silicate layers such as montmorillonite (MMT) have attracted great interest because they frequently exhibit unexpected hybrid properties. A large number of polymers with various degrees of polarity and chain rigidity have been used as polymer matrices for polymer/clay nanocomposites, including polystyrene,[6] polyamides,[7–9] polyimides,[10] epoxy resin,[11] polyure-thane,[12] poly(ethylene terephthalate) (PET),[13] and polypropylene.[14] Li et al.[15] first prepared PBT–clay nanocomposites via melt intercalation with MMT and obtained a good dispersion of the clay layers in the polymer matrix. Then, they studied the effect of the blending sequence on the microstructure and properties of nanocomposites.[16] Chisholm et al.[17] prepared a sulfonated PBT/clay hybrid by polymerization intercalation and studied its morphology and dynamic mechanical properties. However, those studies usually focused on the preparation of PBT/MMT nanocomposites and the characterization of their structure and mechanical properties. No report has been found by the authors on the effect of MMT contents on the crystallization behavior of PBT/MMT nanocomposites in detail.

It is well known that the physical and mechanical properties of crystalline polymers depend on the morphology, crystalline structure, and crystallization degree. The behavior of thermoplastic, semicrystalline polymers during nonisothermal crystallization experiments from their melts is of increasing technological importance because the crystallization conditions are close to the real ones in industrial processes.

Because PBT is a type of semicrystalline polymer and the microstructures of MMT as well as the matrix crystallite may have remarkable effects on the properties of nanocomposites, it is important to study the

influence of MMT on the crystallization process of the matrix. In this study, first the microstructure of PBT/MMT hybrids was characterized with X-ray diffraction (XRD) and transmission electron microscopy (TEM). Then, the nonisothermal crystallization behavior of PBT/MMT hybrids was investigated with differential scanning calorimetry (DSC).

EXPERIMENTAL

Material preparation

The PBT (1097A; number-average molecular weight = 23,200) used in this study was a commercial product of Nantong XinChen Synthetic Material Co., Ltd. (Jiangsu, People's Republic of China). The commercial organic MMT 10A, modified with dimethyl, benzyl, hydrogenated tallow, quaternary ammonium, was provided by South Clay Co. (Gonzales, TX). PBT/MMT nanocomposites were prepared by the direct melt compounding of MMT 10A with PBT in a Rheomix-600 mixer (Rheocord 900, Haake, Germany) at 230°C and 50 rpm for 10 min, and the clay loadings were 1, 3, 6, and 9 wt %, respectively.

Microstructure characterization

The degree of swelling and the interlayer distance of the clay in PBT/MMT were determined by XRD. The experiments were performed with a Rigaku Dmax-rC diffractometer (Tokyo, Japan) with a Cu target and a rotating anode generator operated at 40 kV and 100 mA. The scanning rate was 2°/min from 1 to 10°. The film sample for XRD measurements was prepared via compression molding at 230°C and 10 MPa. TEM micrographs were taken from 80–100-nm-thick microtomed sections with a transmission electron microscope (H-860, Hitachi, Tokyo, Japan) with a 100-kV accelerating voltage.

Nonisothermal crystallization process

Nonisothermal crystallization was carried out on a PerkinElmer Pyris-1 differential scanning calorimeter, and the temperature was calibrated with indium. Samples of the PBT/MMT nanocomposites and PBT, about 0.2 mm thick, were obtained via compression molding at 10 MPa and 230°C and then quenched to room temperature. Disk-like samples (ca. 3 mg) for DSC were cut from the film. In the nonisothermal crystallization process, the samples were melted at 260°C for 10 min to eliminate the previous thermal history and then cooled at constant cooling rates of 5, 10, 20, and 40°C/min. The exothermal curves of heat flow as a function of the temperature were recorded to analyze the nonisothermal crystallization process of the PBT/MMT nanocomposites and PBT. All the experiments were carried out under nitrogen.
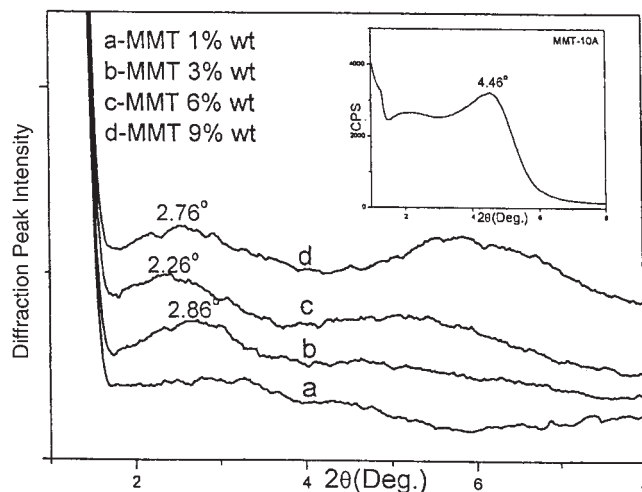
Figure 1 Wide-angle X-ray diffraction patterns for clay and PBT/MMT samples: (a) PBT/MMT1wt%, (b) PBT/MMT3wt%, (c) PBT/MMT6wt%, and (d) PBT/MMT9wt%.

RESULTS AND DISCUSSION

Microstructure of the PBT/MMT nanocomposites

The microstructure of polymer/clay nanocomposites is typically elucidated with XRD and TEM. In XRD patterns, the interlayer spacing of clay can be determined by the site of the peak corresponding to the {001} basal reflection of MMT (called the d_{001} peak). Figure 1 shows the XRD patterns of MMT 10A and PBT/MMT nanocomposites with different MMT loadings. The d_{001} peak of the 10A powder was observed at $2\theta = 4.36°$, and the interlayer distance of the original clay was 1.98 nm. Compared with that of the clay powder, the d_{001} peaks of 10A in the PBT/MMT nanocomposites were dispersed and shifted to lower angles. The interlayer spacing of clay in the nanocomposites with 3, 6, and 9 wt % MMT 10A increased to 3.10, 3.91, and 3.20 nm, respectively, and this indicated that PBT chains diffused into the clay gallery and that the interspacing of silicate layers was swollen to a larger distance. Because the melt intercalation process is controlled by the mass transport of the polymer chain into primary particles of clay, tactoids near the edge may be accessible to the polymer chain.[18] Therefore, it can be inferred that that silicate layers at the end of the silicate stacks may be relatively easy to intercalate or exfoliate. As the clay content approached 9 wt %, the interspacing of silicate layers slightly decreased, and this may have resulted from the obstruction effect on the chain diffusion due to excess silicate.

A TEM study was carried out to confirm the dispersion state of the clay in the matrix. Figure 2(a) presents a TEM image of the PBT/MMT1wt% nanocomposite. The silicate crystallites, or tactoids (dark lines), composed of up to 10 silicate layers, no thicker than 20–30

(a)   (b)

(c)
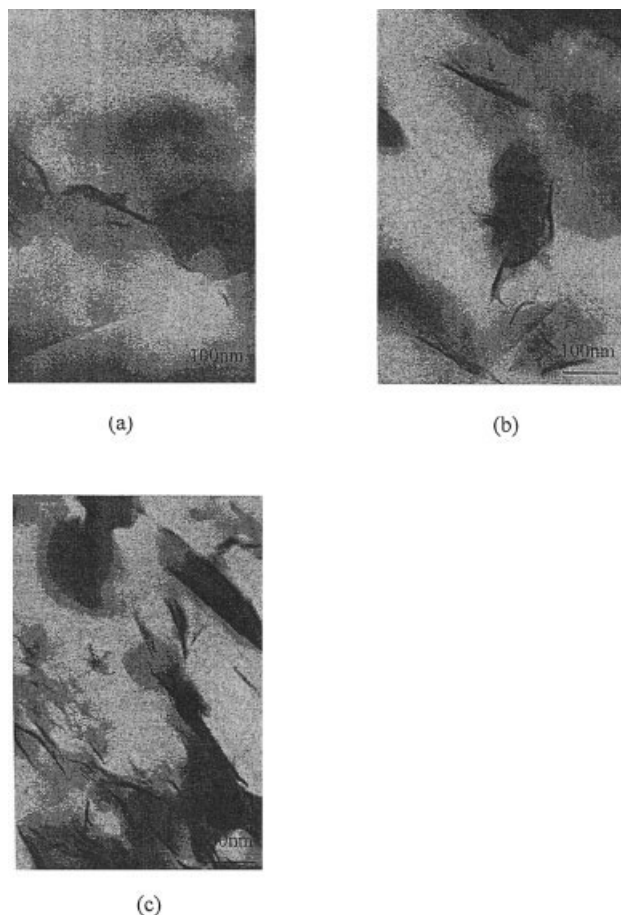
Figure 2 TEM images of PBT/MMT samples: (a) PBT/MMT1wt%, (b) PBT/MMT6wt% at a magnification of 100,000×, and (c) PBT/MMT9wt% at a magnification of 50,000×.

nm, were dispersed in the matrix (white field) in the sample, which showed a partly exfoliated structure. With an increase in the MMT loading, the average thickness of the multilayers broadened, and the layer amounts increased gradually, as shown in Figure 2(b). As the clay content approached 9 wt %, it was observed from Figure 2(c) that the PBT/MMT9wt% sample presented a distinct intercalated structure. Additionally, many fragments of silicate layers were exfoliated from the silicate crystallites as a result of the high shear stresses in the processing. The big particles, intercalated silicate crystallites, and exfoliated layers might have coexisted at the same time, forming a complicated structure. Therefore, the TEM analysis was inconsistent with that of the XRD measurements.

Nonisothermal crystallization behavior

Figure 3(a,b) shows the curves of the heat flow as a function of the temperature during the nonisothermal crystallization of PBT and its nanocomposite at different cooling rates, respectively. As the cooling rate

increased from 5 to 40°C/min, the exothermic peak temperature decreased from 198.3 to 184.3°C, and the exotherms became broader. Thus crystallization occurred at lower temperatures with faster cooling rates. In addition, the molecular chains became less flexible and less mobile and had less time to diffuse into the crystallite lattice and to adjust and organize the chain configurations into more perfect crystallites. As a result, the extent of crystallite perfection also decreased with faster cooling rates. A similar trend could be observed in Figure 3(b) for the PBT/MMT hybrid.

It is well accepted that clay layers may serve as additional nucleation sites that will accelerate nucleation and raise the crystallization temperature. To find out the effect of the clay content on the crystallization behavior of PBT, the curves of the heat flow as a function of the temperature during the nonisothermal crystallization for nanocomposites with different MMT loadings at the same cooling rates are shown in

(a)

(b)
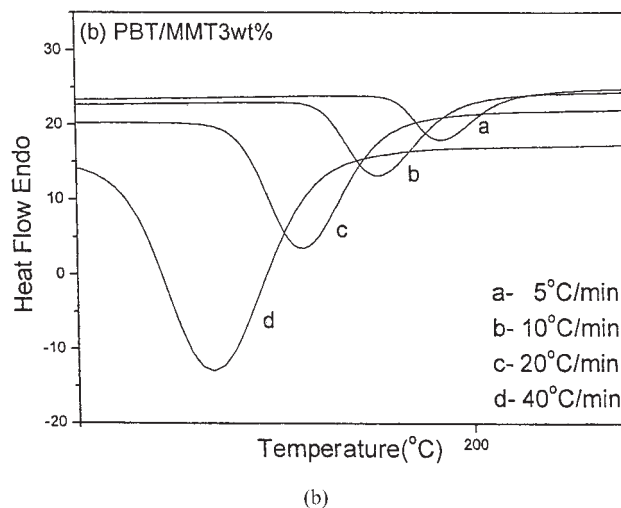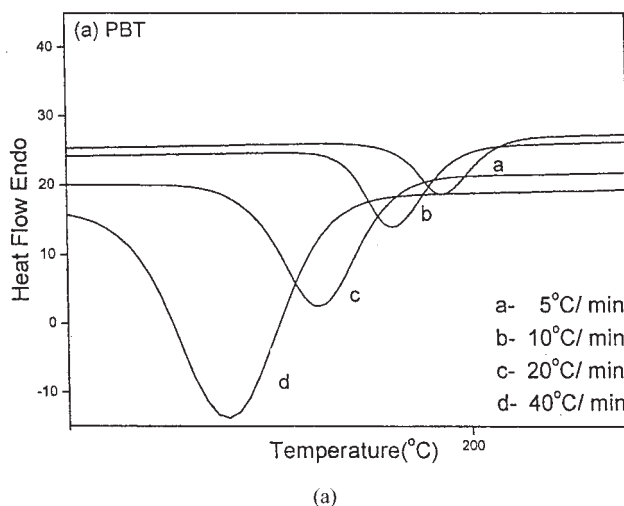
Figure 3 Curves of the heat flow versus the temperature at different cooling rates for (a) PBT and (b) PBT/MMT3wt%.
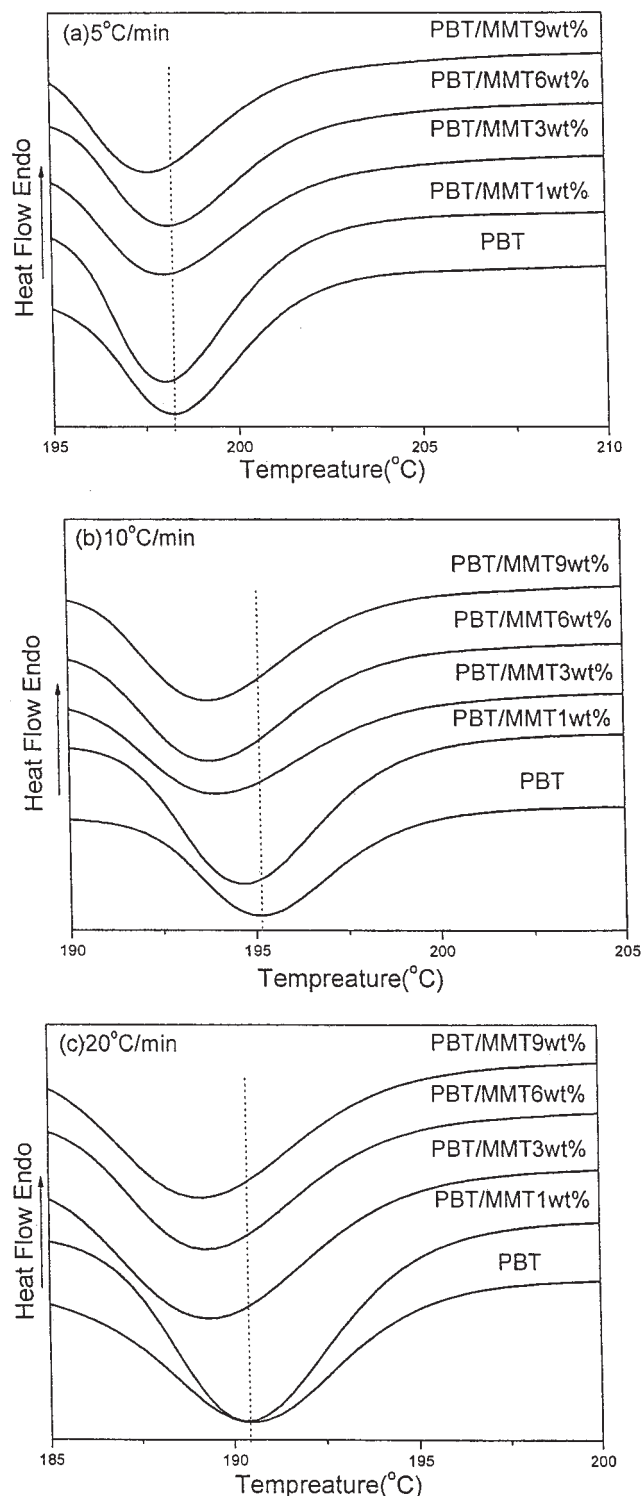
Figure 4 Curves of the heat flow versus the temperature with different MMT contents at the same cooling rates: (a) 5, (b) 10, (c) 20.

Figure 4. Surprisingly, compared with that for pure PBT, the exothermic peaks for the nanocomposites distinctly shifted to lower temperatures at various cooling rates, and with an increase in the MMT content, the peak crystallization temperature of the PBT/

MMT hybrids declined gradually. This suggests that the presence of clay particles may prevent large crystalline domains from forming because of limited space and restrictions imposed on polymer chains. A similar decreasing trend in the peak crystallization temperature was found in polyamide 6 PA6/MMT nanocomposites with the DSC method,[19–22] and they attributed this trend to the physical hindrance of MMT layers to the motion of polymer molecular chains. In other words, the lower peak crystallization temperature observed in the nanocomposites resulted from the inability of polymer molecular chains to be fully incorporated into growing crystalline lamella.

Chisholm et al.[17] studied the isothermal crystallization of PBT ionomer/clay and found that the addition of clay slightly decreased the rate of crystallization. They thought that clay particles were not effective nucleating agents for PBT crystallization, and the decrease in the crystallization rate might be attributed to an increase in the viscosity of the melt. On the basis of isothermal crystallization results, Fornes and Paul[19] reported that the half-time of crystallization ($t_{1/2}$) of PA6/MMT nanocomposites containing ≤1.5 wt % MMT was lower than that of pristine PA6. $t_{1/2}$ tended to increase monotonically when the MMT concentration was ≥2 wt %. A decrease in the degree of crystallinity had also been reported to occur in polyethylene/clay and poly(vinylidene fluoride)/clay nanocomposites.[23,24] In our previous work, the isothermal crystallization of PBT/MMT nanocomposites was studied.[25] The results clearly indicated that very small amounts of clay (1 wt %) could effectively increase the rate of crystallization, whereas higher clay loadings reduced the rate of crystallization at the lower crystallization temperature, as shown in Figure 5(a). However, Figure 5(b) shows that at the higher crystallization temperature, even the crystallization of the PBT/MMT nanocomposites with a lower clay loading (1 wt %) was slower than that of pure PBT. Therefore, it can be concluded that MMT clay plays two roles in the crystallization of the matrix: it acts as a heterogeneous nucleating agent to facilitate crystallization and as a physical hindrance to retard crystallization. Which role of MMT is dominant depends on both the MMT content and the crystallization behavior of the matrix itself. These two factors might affect the nonisothermal crystallization behavior of PBT/MMT nanocomposites likewise.

Nonisothermal crystallization kinetics

To further analyze the nonisothermal crystallization process, the nonisothermal crystallization kinetics of PBT and its hybrids were compared. Several methods have been developed to describe the nonisothermal crystallization kinetics of polymers. For example,
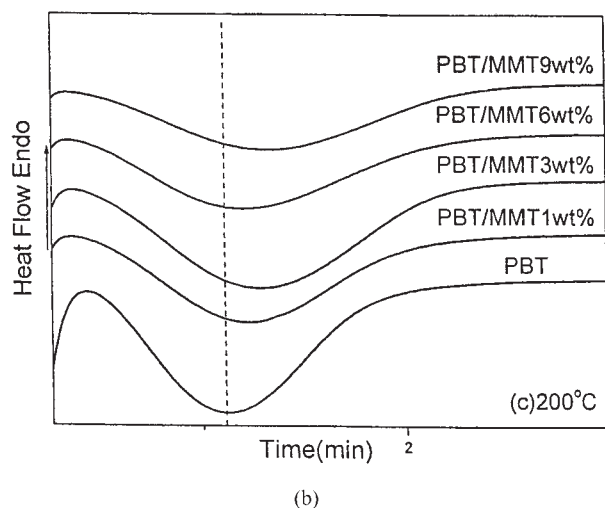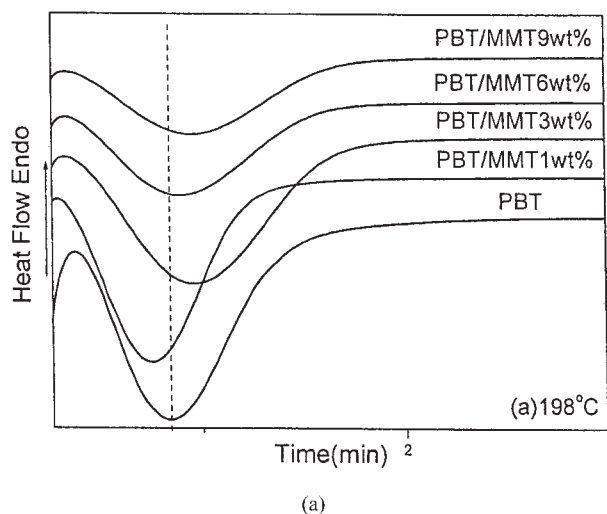
Figure 5 Curves of the heat flow versus the time for nanocomposites with different MMT loadings at identical crystallization temperatures: (a) 198 and (b) 200°C.

nonisothermal crystallization can be directly analyzed by the Avrami equation:[26]

$$X(t) = 1 - \exp(-Kt^n) \tag{1}$$

$$\log[-\ln[1-X(t)]] = n\log t + \log K \tag{2}$$

where $X(t)$ is the relative crystallinity at crystallization time t, n is the Avrami exponent, and K is the crystallization rate constant changing with temperature. Figure 6 presents curves of the relative crystallinity as a function of temperature during nonisothermal crystallization for nanocomposite with different MMT loadings at the same cooling rates. As shown in Figure 6(a), the PBT/MMT nanocomposites had a slightly faster crystallization rate than that of the matrix in the beginning of the crystallization process at the lower cooling rate (−5°C/min). However, with the growth

of the crystal, only the PBT/MMT nanocomposites with clay concentrations of 1–3 wt % showed a faster crystallization rate. When the cooling rate approached −20°C/min, only the PBT/MMT1wt% nanocomposite presented a higher crystallization rate, as can be seen in Figure 6(b). These curves reiterated that on the one hand, very small amounts of clay could increase the rate of crystallization, whereas higher clay loadings retarded crystallization; this was in agreement with the results for the isothermal crystallization behavior.[25] On the other hand, the cooling rate might have an influence on the crystallization process of the hybrids.

TEM images showed that with an increase in the MMT loadings, the exfoliation degree of clay declined, and the size of the silicate multilayers in the nanocomposites became larger. Therefore, as at a lower clay concentration, the distance between the clay layers was large enough for it to be relatively easy for the
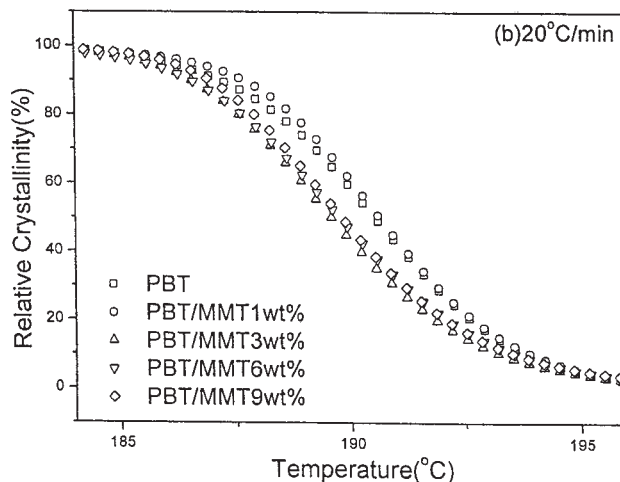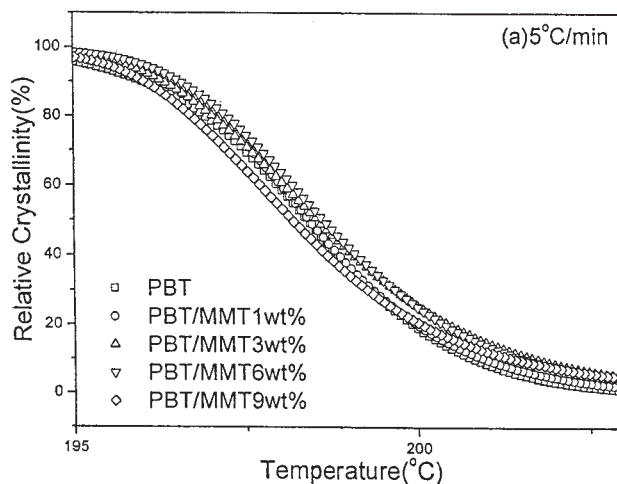
Figure 6 Curves of the relative crystallinity versus the temperature with different MMT loadings at the same cooling rates: (a) 5 and (b) 20°C/min.

additional nucleation sites to incorporate surrounding polymer, and the crystal nucleus formed easily, especially at a lower cooling rate. In this case, the role of MMT as an additional nucleation agent was dominant. However, with an increase in the MMT loadings, the diffusion of polymer chains to the growing crystallite was hindered by large amounts of clay particles, despite the formation of some additional nucleation sites. Moreover, at the higher cooling rate, the PBT molecular chains became less flexible and less mobile and had less time to diffuse into the crystallite lattice; thus, the hindrance effect of clay particles even at a lower concentration on the polymer chains was stronger than the nucleating effect, which retarded the crystal growth process.

In the nonisothermal crystallization process, t can be determined as follows:

$$t = \frac{T_0 - T}{\phi} \tag{3}$$

where ϕ is the cooling rate, T is the temperature at crystallization time t, and T_0 is the initial crystallization temperature. Figure 7 shows the development of $X(t)$ of PBT and its nanocomposite with t at different cooling rates, indicating that the time for completion of crystallization could be reduced by an increase in the cooling rate. Plots of $\log\{-\ln[1 - X(t)]\}$ versus $\log t$ are shown in Figure 8. Each curve shows only the linear portion, and the nonlinear part that deviated from the Avrami equation at a high relative crystallinity region was not included. Small deviations from linearity in the short-time region, in which logarithmic plotting tended to exaggerate small errors in the assignment of the start of crystallization, were also removed to show the proportional region more clearly.[27] According to eq. (2), by the plotting of $\log\{-\ln[1 - X(t)]\}$ versus $\log t$, the kinetic parameter n was obtained from the slope of the line, and it is presented in Table I. A narrow spread of n values of PBT centered at 4.0 was obtained. The results indicated that the crystals in the pure PBT melt showed mostly spherulitic growth, and the nucleation process was homogeneous under the experimental conditions. At the same cooling rate, the n values decreased slightly with the addition of clay, and this indicated that although the silicate layers had a heterogeneous nucleating effect on PBT to some extent, the homogeneous nucleation of PBT itself was dominant in the crystallization process. Tjong and Bao[22] reported a similar result for the nonisothermal crystallization behavior of PA6–clay nanocomposites. They thought that the MMT platelets did not promote the nucleation of the PA6 crystallites because the addition of MMT to PA6 had little influence on the folded surface energy.

Ozawa[28] developed the Avrami method to deal with the nonisothermal crystallization process. If we
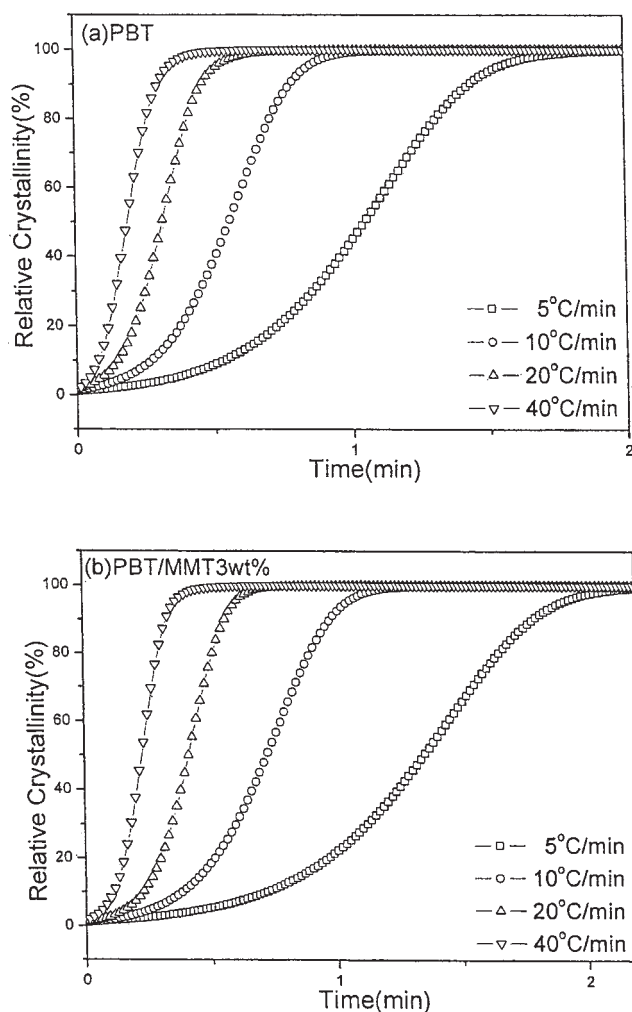
Figure 7 $X(t)$ versus t at different cooling rates: (a) 5 and (b) 20°C/min.

presume that the nonisothermal crystallization process is composed of many infinitesimal isothermal ones, the kinetic equation can be described as follows:

$$X(T) = 1 - \exp[-K(T)/\phi^m] \tag{4}$$

From eq. (4), it follows:

$$\ln\{-\ln[1 - X(T)] = \ln K(T) - m\ln\phi \tag{5}$$

where $X(T)$ is a cooling function and m is the Ozawa exponent. Plots of $\ln\{-\ln[1 - X(t)]\}$ versus $\ln \phi$ for the PBT/MMT3wt% and PBT/MMT9wt% hybrids are shown in Figure 9(a,b), respectively. Apparently, the nice linearity of these curves suggests that the Ozawa model provided a satisfactory description of the nonisothermal melt crystallization for these hybrids at lower and higher clay loadings.

Considering the influence of various cooling rates on the nonisothermal crystallization process, Jezi-
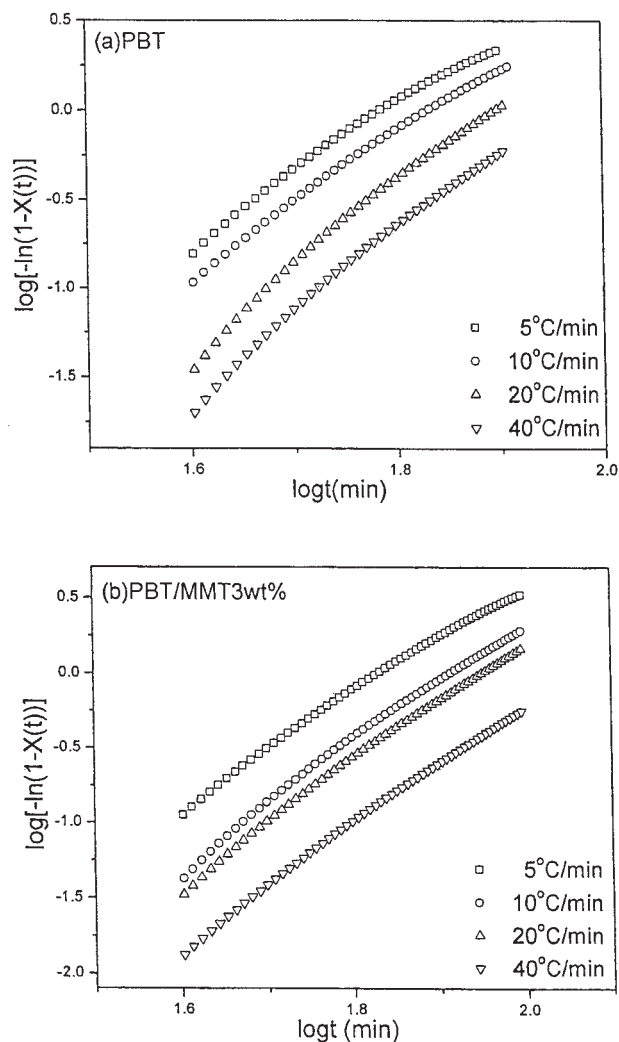
Figure 8 Plots of $\log\{-\ln[1 - X(t)]\}$ versus $\log t$ for nonisothermal crystallization: (a) PBT and (b) PBT/MMT3wt%.

oney[29] gave the final form of the parameter characterizing the kinetics during nonisothermal crystallization as follows:

$$\ln Z_c = \ln Z_t / \phi \tag{6}$$

where Z_t is the crystallization rate constant and Z_c is the modified crystallization rate constant with respect to ϕ. The results obtained from Avrami plots and with the Jeziorny method are listed in Table I. As expected, $t_{1/2}$ decreased with an increase in the cooling rates for PBT and the PBT/MMT hybrids. Moreover, at a given cooling rate, the values of $t_{1/2}$ for the PBT/MMT hybrids with a clay concentration of 1 wt % were smaller than that of pure PBT, whereas those samples with higher clay loadings presented a larger value. These results further proved that very small amounts of clay could accelerate the crystallization process, whereas higher clay loadings retarded the crystal growth process.

Ke et al.[13] studied PET/MMT hybrids and observed a dramatic advance in the crystallization rate with increasing clay loadings; this was a totally different crystallization behavior from that for PBT/MMT nanocomposites. $t_{1/2}$ of PET was about 2 times longer than that of PBT under the same experimental conditions, and this indicated that PET exhibited worse crystallization behavior because its molecular chains were less flexible and less mobile than those of PBT. Therefore, the nucleating effect by silicate layers on the PET/MMT hybrids may have a dominant role. However, the pure PBT showed a good homogeneous nucleation process because of its higher chain flexibility and mobility. Accordingly, in comparison with the additional nucleating effect, a physical hindrance effect by higher clay loadings was more remarkable in the PBT/MMT hybrids. Therefore, the nature of the matrix itself also affected the crystallization behavior of the polymer/clay nanocomposites.

Recently, a new approach was developed by Mo et al.[30] to study the nonisothermal crystallization of crystalline and semicrystallization polymers. For the nonisothermal crystallization process, physical variables relating to the process are the relative degree of crystallinity (X_t), ϕ, and T. Both the Ozawa and Avrami equations give their relationship as follows:

$$\ln Z_t + n\ln t = \ln K(T) - m\ln\phi \tag{7}$$

By a rearrangement at a certain value of X_t

$$\ln\phi = \ln F(T) - \alpha\ln t \tag{8}$$

TABLE I
Parameters from the Avrami and Jezioney Analysis

Sample	ϕ (°C/min)	n	Z_c	$t_{1/2}$ (min)
PBT	5	4.05	0.66	1.20
	10	3.93	1.03	0.81
	20	3.86	1.22	0.40
	40	3.76	1.56	0.28
PBT/MMT1wt%	5	4.10	0.71	1.18
	10	3.91	1.08	0.75
	20	3.82	1.25	0.36
	40	3.76	1.67	0.28
PBT/MMT3wt%	5	3.95	0.58	1.42
	10	3.76	0.95	0.98
	20	3.75	1.08	0.75
	40	3.65	1.40	0.32
PBT/MMT6wt%	5	4.02	0.54	1.75
	10	3.88	0.95	1.10
	20	3.68	1.05	0.60
	40	3.46	1.38	0.32
PBT/MMT9wt%	5	3.95	0.49	1.85
	10	3.75	0.87	1.26
	20	3.77	0.99	0.61
	40	3.58	1.33	0.33
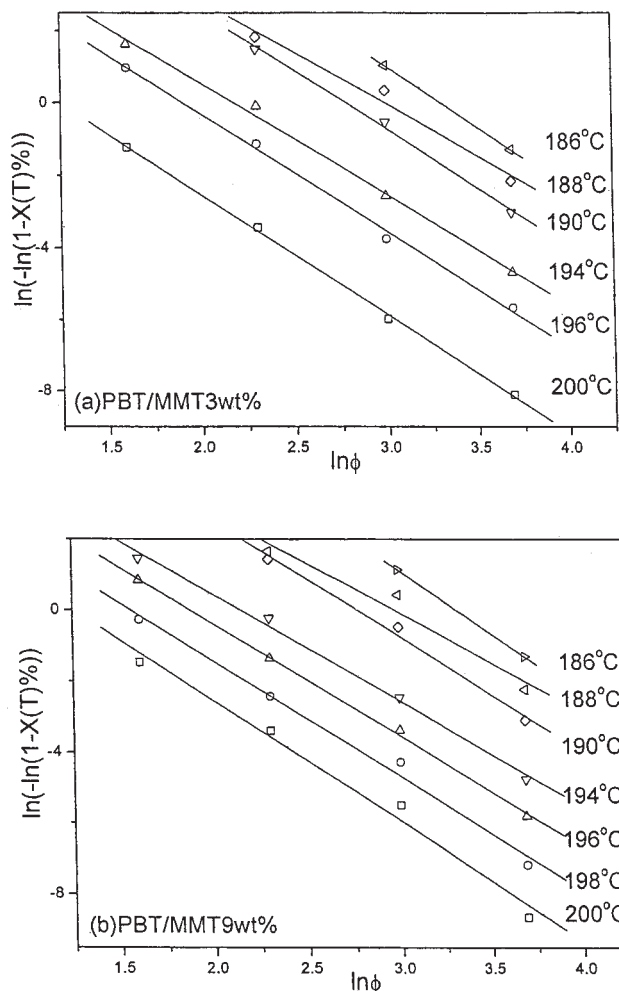
Figure 9 Plots of $\ln\{-\ln[1 - X(t)]\}$ versus $\ln \phi$ for nonisothermal crystallization: (a) PBT/MMT3wt% and (b) PBT/MMT9wt%.

where $F(T) = [K(T)/Z_t]^{1/m}$ refers to the value of the cooling rate, which must be chosen within the unit of t when the measured system amounts to a certain degree of crystallinity. α is equal to n/m. According to eq. (6), at a given degree of crystallinity, plotting $\ln \phi$ versus $\ln t$ (Fig. 10) yields a linear relationship between $\ln \phi$ and $\ln t$. The kinetic parameter $F(T)$ and α were determined from the intercept and slope of the lines. They are listed in Table II for PBT and its hybrids.

Table II shows that the values of α changed from 1.12 to 1.13 for PBT and from 1.12 to 1.14 for its hybrids. The values of $F(T)$ increased monotonously with X_t. It was also obvious that for a certain X_t value, the value of $F(T)$ for the PBT/MMT1wt% hybrid was smaller than that for pristine PBT; that is, with the identical X_t value being approached, the PBT/MMT1wt% hybrid required a smaller cooling rate. In other words, the hybrid with a 1 wt % concentration crystallized at a higher rate than PBT. However, the values of $F(T)$ for those hybrids with higher MMT

loadings (≥ 3 wt %) were larger than that for pristine PBT, and this meant that the addition of clay retarded the crystallization of the matrix. The results agreed with those drawn from Avrami analysis and Jezioney analysis.

Kissinger[31] suggested a method for determining the activation energy for the transport of the macromolecular segments to the growing surface (ΔE) by calculating the variation of T_p with ϕ:

$$\frac{d[\ln(\phi/T_p^2)]}{d(1/T_p)} = \frac{-\Delta E}{R} \tag{9}$$

where R is the gas constant and T_p is the temperature corresponding to the peak temperature of DSC crystallization curves. The values of ΔE are listed in Table II. The results clearly indicated that the hybrids with small amounts of clay (≤ 3 wt %) presented lower activation energies than PBT, whereas those with
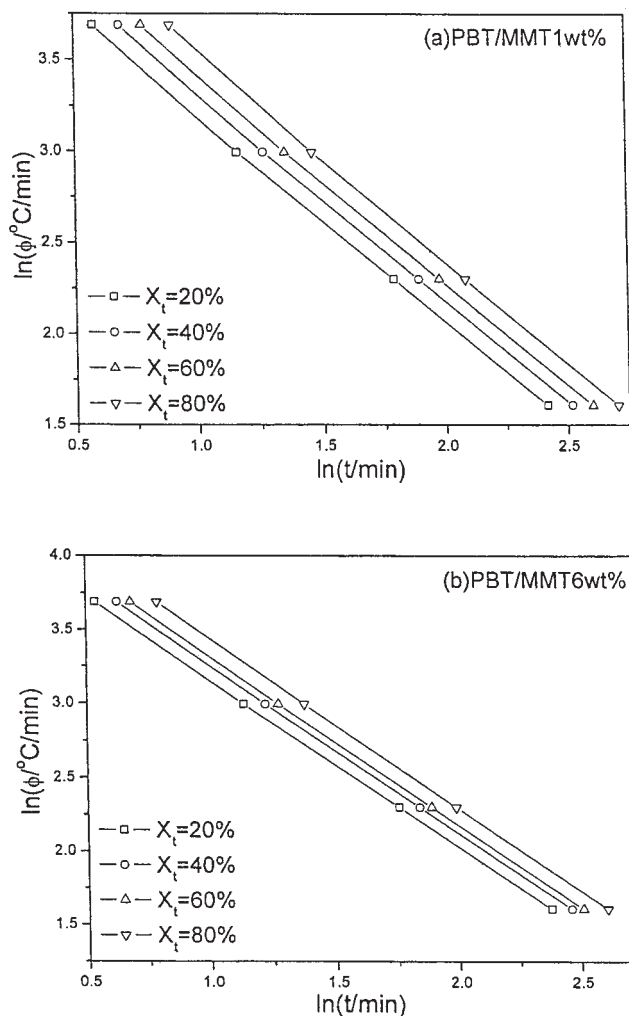
Figure 10 Linear relationship between $\ln \phi$ and $\ln t$ for PBT/MMT nanocomposites with different clay contents: (a) 1 and (b) 6 wt %.

TABLE II
Parameters from the Mo and Kissinger Analysis

Sample	X (%)	F(T)	α	ΔE (kJ/mol)
PBT	d20	4.40	1.12	275
	40	4.42	1.13	
	60	4.45	1.13	
	80	4.48	1.13	
PBT/MMT1wt%	20	4.40	1.12	262
	40	4.41	1.12	
	60	4.45	1.13	
	80	4.46	1.14	
PBT/MMT3wt%	20	4.42	1.13	273
	40	4.41	1.12	
	60	4.48	1.14	
	80	4.50	1.14	
PBT/MMT6wt%	20	4.41	1.13	279
	40	4.45	1.13	
	60	4.48	1.14	
	80	4.51	1.14	
PBT/MMT9wt%	20	4.42	1.13	286
	40	4.45	1.13	
	60	4.47	1.13	
	80	4.50	1.14	

higher clay loadings showed the opposite. A similar variation trend of ΔE with the clay loadings was observed for the isothermal crystallization process,[25] and this further proved that the clay loadings and crystallization conditions as well as the nature of the matrix itself affected the crystallization behavior of the nanocomposites.

CONCLUSIONS

Investigations of polymer crystallization behavior were carried out for PBT/MMT nanocomposites formed by melt processing. Nonisothermal crystallization experiments were used to evaluate the influence of the clay concentration and crystallization conditions on the kinetics of polymer crystal formation. The results showed that the exothermic peaks for the nanocomposites distinctly shifted to lower temperatures at various cooling rates compared with that for pure PBT, and with increasing MMT content, the peak crystallization temperature of the PBT/MMT hybrids declined gradually. The Avrami, Jeziorny, Ozawa, and Mo methods were successful in describing the nonisothermal crystallization process of PBT and its hybrids. The difference in the nonisothermal kinetic parameters between the nanocomposites and polymer matrix showed that very small amounts of clay could effectively accelerate the crystallization process, whereas higher clay loadings reduced the rate of crystallization; this indicated that the MMT loadings had a distinct effect on the crystallization behavior of the nanocomposites. The MMT clay played two roles in the crystallization of the matrix: it acted as a heterogeneous nucleating agent to facilitate crystallization and as a

physical hindrance to retard crystallization. Moreover, the crystallization conditions, such as the cooling rate and the nature of the polymer matrix itself, could affect the crystallization behavior of the nanocomposites, too. At a higher cooling rate ($-20°C/min$), the PBT molecular chains became less flexible and less mobile and had less time to diffuse into the crystallite lattice; thus, the hindrance effect of clay particles on polymer chains was stronger than the nucleating effect. Therefore, only the nanocomposite with a much lower addition of clay (1 wt %) presented a higher crystallization rate. Furthermore, PBT/MMT nanocomposites with lower concentrations of clay (1–3 wt %), which were determined by the Kissinger method, showed lower activation energies than PBT, whereas those with higher clay loadings showed higher activation energies.

References

1. Kim, J. K.; Lee, H. Y. Polymer 1996, 37, 305.
2. Sun, Y. J.; Hu, G. H.; Lambla, M. Polymer 1996, 37, 4119.
3. Park, C. S.; Lee, K. J.; Kim, S. W.; Lee, Y. K.; Nam, J. D. J Appl Polym Sci 2002, 86, 478.
4. Jang, J.; Won, J. Polymer 1998, 39, 4335.
5. Ou, C. F.; Chao, M. S.; Huang, S. L. J Eur Polym 2000, 36, 2665.
6. Vaia, R. A.; Jandt, K. D.; Kramer, E. J.; Giannelis, E. P. Chem Mater 1996, 8, 2628.
7. Kojima, Y.; Usuki, A. M.; Kawasumi, A.; Okada, T.; Kurauchi, A.; Kamigaito, O. J Polym Sci Part A: Polym Chem 1993, 31, 983.
8. Wu, Z. G.; Zhou, C. X.; Qi, R. R.; Zhang, H. B. J Appl Polym Sci 2002, 83, 2403.
9. Wu, Z. G.; Zhou, C. X. Polym Test 2002, 21, 479.
10. Tyan, H. L.; Liu, Y. C.; Wei, K. H. Polymer 1999, 40, 4877.
11. Lan, T.; Kaviratna, P. D.; Pinnavaia, T. J. J Phys Chem Solids 1996, 57, 6.
12. Ma, J.; Zhang, S.; Qi, Z. N. J Appl Polym Sci 2001, 2, 1444.
13. Ke, Y. C.; Long, C. F.; Qi, Z. N. J Appl Polym Sci 1999, 71, 1139.
14. Li, J.; Zhou, C. X.; Wang, G. Polym Test 2002, 21, 332.
15. Li, X. C.; Kang, T. K.; Cho, W. J. Macromol Rapid Commun 2001, 22, 1306.
16. Li, X. C. Polym Eng Sci 2002, 42, 2156.
17. Chisholm, B. J.; Moore, R. B.; Barber, G.; Khouri, F.; Hempstead, A.; Larsen, M. Macromolecules 2002, 35, 5508.
18. Vaia, R. A.; Janndt, D. K.; Kramer, E. J. Macromolecules 1995, 28, 8080.
19. Fornes, T. D.; Paul, D. R. Polymer 2003, 44, 3945.
20. Lincon, D. M.; Vaia, R. A.; Wang, Z. G.; Hsiao, B. S. Polymer 2001, 42, 1621.
21. Liu, X.; Wu, Q.; Berglund, L. A.; Qi, Z. Macromol Mater Eng 2002, 287, 515.
22. Tjong, S. C.; Bao, S. P. J Polym Sci Part B: Polym Phys 2004, 42, 2878.
23. Gopakumar, T. G.; Lee, J. A.; Kontopoulou, M.; Parent, J. S. Polymer 2002, 43, 5483.
24. Priya, L.; Jog, J. P. J Polym Sci Part B: Polym Phys 2002, 40, 1682.
25. Wu, D. F.; Zhou, C. X.; Xie, F.; Mao, D. L.; Zhang, B. Polym Polym Compos 2005, 13, 61.
26. Herrero, C. R.; Acosta, J. L. Polym J 1994, 26, 786.
27. Seo, Y.; Kim, J.; Kim, K. U.; Kim, Y. C. Polymer 2000, 41, 2639.
28. Ozawa, T. Polymer 1971, 12, 150.
29. Jeziorny, A. Polymer 1978, 19, 1142.
30. Liu, T. X.; Mo, Z. S.; Wang, S.; Zhang, H. F. Polym Eng Sci 1997, 37, 568.
31. Kissinger, M. J Res Natl Stand 1956, 57, 217.